

Engineering flexible machine learning systems by traversing functionally-invariant paths

Guruprasad Raghavan,¹ Matt Thomson,^{1*}

¹Department of Bioengineering, Caltech
1200 E California Blvd, Pasadena, CA 91125

*To whom correspondence should be addressed;
mthomson@caltech.edu
graghava@caltech.edu

Abstract

Deep neural networks achieve human-like performance on a variety of perceptual and decision-making tasks. However, networks perform poorly when confronted with changing tasks or goals, and broadly fail to match the flexibility and robustness of human intelligence. Here, we develop a mathematical and algorithmic framework that enables flexible and continuous training of neural networks on a range of objectives by constructing path connected sets of networks that achieve equivalent functional performance on a given machine learning task. We view the weight space of a neural network as a curved Riemannian manifold and move a network along a functionally invariant path in weight space while searching for networks that satisfy secondary objectives. A path-sampling algorithm trains computer vision and natural language processing networks with millions of weight parameters to learn a series of classification tasks without performance loss while accommodating secondary objectives including network sparsification, incremental task learning, and increased adversarial robustness. Broadly, we conceptualize a neural network as a mathematical object that can be iteratively transformed into distinct configurations by the path-sampling algorithm to define a sub-manifold of networks that can be harnessed to achieve user goals.

Introduction

Artificial neural networks out-perform humans on tasks ranging from image recognition and game playing to protein structure prediction [1, 2, 3]. However, artificial neural networks fail to replicate the flexibility and robustness of human intelligence [4, 5, 6]. Humans can learn new tasks and accommodate novel goals with minimal instruction and without loss of performance on existing tasks. Unlike humans, deep neural networks suffer catastrophic forgetting, or significant performance decay, when trained to perform additional tasks or integrate new information [7, 8]. For example, a network trained to recognize images of hand-written digits [9] will ‘forget’ the digit recognition task when trained to recognize additional objects like letters or faces. In addition to well-known flexibility limits, deep neural networks have other pathologies, like vulnerability to targeted corruption of input data or adversarial fragility where small, imperceptible changes in the input data can cause complete failure of network performance.

In artificial neural networks, network function is encoded in the mathematical weights that determine the strength of connections between neural units (Fig. 1). Deep learning procedures train multi-layered neural networks to solve problems by adjusting the weights of a network based on an objective function that encodes the performance of a network on a specific task. Standard learning methods, like back-propagation and gradient descent [10], adjust network weights to define a single, optimal weight configuration to maximize performance on a task specific objective function using training data. Training the network on new tasks through the traditional paradigm of stepping

along the gradient of the task-specific objective function adjusts the networks’ weights, inevitably resulting in the loss of information from previous tasks.

The weight adjustment problem underlies other challenges in modern machine learning. For example, it is advantageous to prune or sparsify a network to minimize the number of non-zero weights and thus reduce network memory and power consumption. Just like multi-task learning, network sparsification requires the adjustment of network weights while maintaining function, and sparsification procedures often proceed through heuristic weight pruning strategies. For adversarial robustness, a central goal is to identify ensembles of networks that perform a task with distinct weight configurations and thus avoid vulnerabilities associated with a single weight configuration.

Unlike contemporary artificial neural nets, neural networks in the human brain perform multiple functions and can flexibly switch between different functional configurations based on context, goals or memory [11]. Neural networks in the brain are hypothesized to overcome the limitations of a single, optimal weight configuration and perform flexible tasks by continuously ‘drifting’ their neural firing states and neural weight configurations, effectively generating large ensembles of degenerate networks [12, 13]. Fluctuations might enable flexibility in biological systems by allowing neural networks to explore a series of network configurations while responding to sensory input.

Here, we develop a geometric framework and algorithm to construct path connected sets of neural networks that solve a given machine learning task. Conceptually, we consider path-connected sets of neural networks, rather than single-networks (isolated points in weight space) to be the central objects of study and application. By building sets of networks rather than single networks, we search within a sub-manifold of weight space for networks that solve a given machine learning problem while accommodating a broad range of secondary goals. We view a neural networks’ weight space as a Riemannian manifold equipped with a distance metric that represents task performance. Our core algorithm identifies functionally invariant paths in weight space that maintain network performance while ‘searching-out’ for other networks that satisfy additional objectives like sparsification or mitigating catastrophic interference. We demonstrate that the path sampling algorithm achieves high performance on a series of meta-tasks: sequential task learning, network sparsification, and adversarial robustness on a range of vision and language networks with millions of parameters obtaining performance similar to domain specific approaches.

Construction of functionally invariant paths in weight space

We develop a mathematical framework that allows us to define and explore path-connected sets of neural networks that have divergent weight values but similar output on training data. We view the weight-space of a neural network as a Riemannian manifold equipped with a local distance metric [14, 15]. Using differential geometry, we construct paths through weight space that maintain the functional performance of a neural network while adjusting network weights to flow along a secondary goal. The secondary goal can be general, so that the framework can be applied to train networks on new classification tasks, to sparsify networks, and also to mitigate adversarial fragility.

The defining feature of a Riemannian manifold is the existence of a local distance metric. We construct a distance metric in weight space that defines the distance between two nearby networks to be their difference in output. We consider a neural network to be a smooth function, $f(\mathbf{x}; \mathbf{w})$, that maps an input vector, $\mathbf{x} \in \mathbb{R}^k$, to an output vector, $f(\mathbf{x}; \mathbf{w}) = \mathbf{y} \in \mathbb{R}^m$, where the map is parameterized by a vector of weights, $\mathbf{w} \in \mathbb{R}^n$, that are typically set in training to solve a specific task. We refer to $W = \mathbb{R}^n$ as the *weight space* of the network, and we refer to $\mathcal{Y} = \mathbb{R}^m$ as the *output space* as shown in Fig. 1B [16]. For pedagogical purposes, we will consider the action of f on a single input, \mathbf{x} . In the supplement we show that our results extend naturally to an arbitrary number of inputs \mathbf{x}_i (Supporting Information).

We initially ask how the output, $f(\mathbf{x}; \mathbf{w})$, of a given neural network changes for small changes

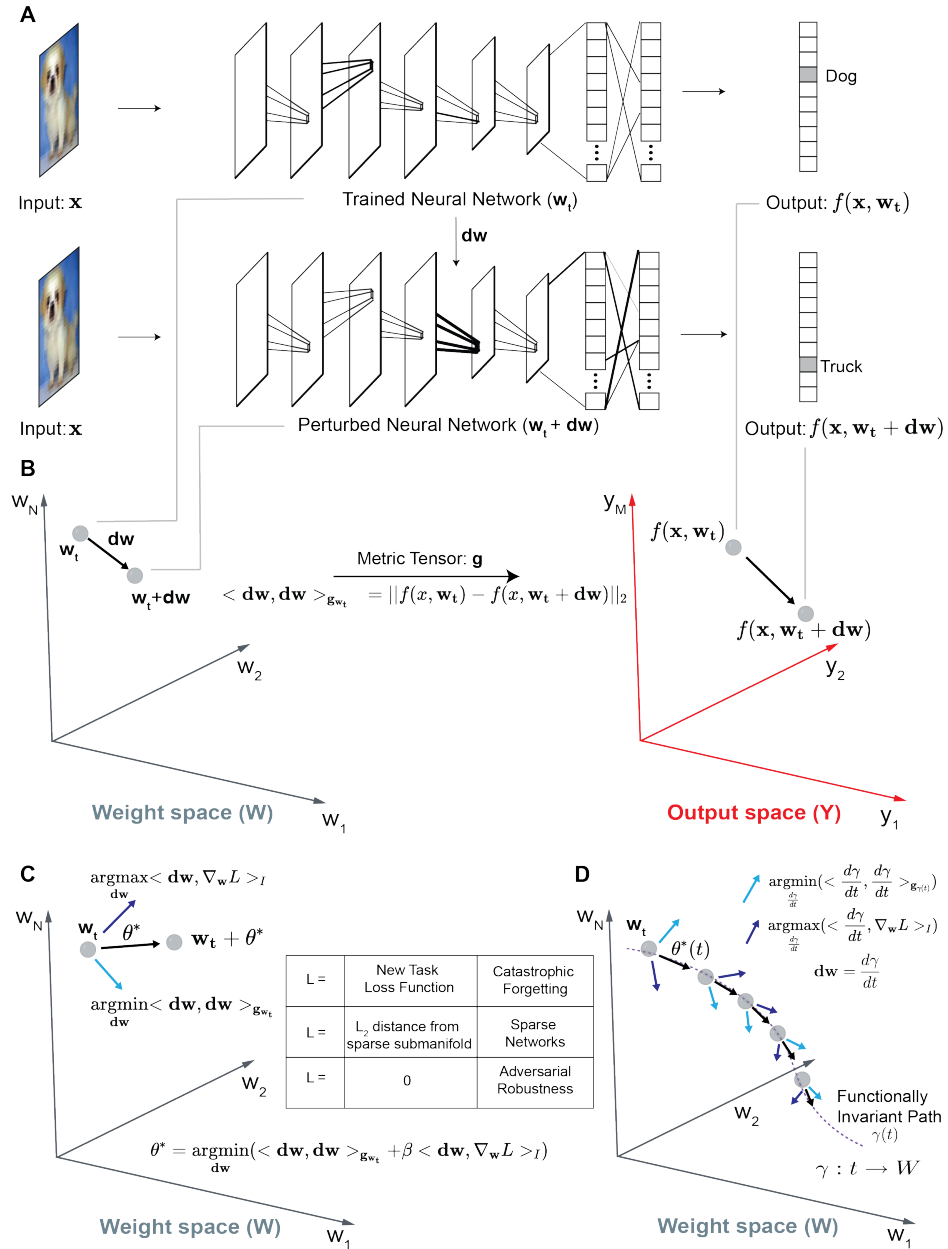


Figure 1: **Geometric Framework for constructing functionally invariant paths (FIP) in weight space.** (A) (Top) A trained convolutional neural network with weight configuration (\mathbf{w}_t), represented by lines connecting different layers of the network, accepts an input image, \mathbf{x} , and produces a 10-element output vector, $f(\mathbf{x}, \mathbf{w}_t)$. (Below) Perturbation of network weights by $\mathbf{d}\mathbf{w}$ results in a new network with weight configuration $\mathbf{w}_t + \mathbf{d}\mathbf{w}$ with an altered output vector, $f(\mathbf{x}, \mathbf{w}_t + \mathbf{d}\mathbf{w})$, for the same input, \mathbf{x} . (B) Mathematically, perturbation of the networks' weight configuration shift the network from \mathbf{w}_t to $\mathbf{w}_t + \mathbf{d}\mathbf{w}$ in weight space (W). The network's output, $f(\mathbf{x}, \mathbf{w}_t)$, shifts to $f(\mathbf{x}, \mathbf{w}_t + \mathbf{d}\mathbf{w})$ in output space (Y). The metric tensor ($\mathbf{g}_{\mathbf{w}_t}$) transforms perturbation in weight space ($\mathbf{d}\mathbf{w}$) to distance moved in the output space ($\|f(\mathbf{x}, \mathbf{w}_t) - f(\mathbf{x}, \mathbf{w}_t + \mathbf{d}\mathbf{w})\|_2$). (C) The FIP algorithm identifies weight perturbations, θ^* that minimize distance moved in output space while maximizing alignment with gradient of a secondary objective function ($\nabla_{\mathbf{w}} L$). The light-blue arrow indicates ϵ -norm weight perturbation that minimizes distance moved in output space, dark-blue arrow is ϵ -norm weight perturbation that maximizes alignment with gradient of objective function, $L(\mathbf{x}, \mathbf{w})$. The secondary objective function $L(\mathbf{x}, \mathbf{w})$ is varied to solve distinct machine learning challenges. (D) The path algorithm defines functionally invariant paths, $\gamma(t)$, through iterative identification of ϵ -norm perturbations ($\theta^*(t)$) in the weight space.

in network weights. Given a neural network with weights \mathbf{w}_t , a fixed input \mathbf{x} , we can compute the output of the perturbed network, $\mathbf{w}_t + \mathbf{dw}$ for an infinitesimal weight perturbation, \mathbf{dw} as

$$f(\mathbf{x}, \mathbf{w}_t + \mathbf{dw}) \approx f(\mathbf{x}, \mathbf{w}_t) + \mathbf{J}_{\mathbf{w}_t} \mathbf{dw}, \quad (1)$$

where $\mathbf{J}_{\mathbf{w}_t}$ is the Jacobian of $f(\mathbf{x}, \mathbf{w}_t)$ for a fixed \mathbf{x} , $J_{ij} = \frac{\partial f_i}{\partial w_j}$, evaluated at \mathbf{w}_t .

Thus, the total change in network output for a given weight perturbation \mathbf{dw} is

$$\begin{aligned} |f(\mathbf{x}, \mathbf{w}_t + \mathbf{dw}) - f(\mathbf{x}, \mathbf{w}_t)|^2 &= \mathbf{dw}^T (\mathbf{J}_{\mathbf{w}_t}(\mathbf{x})^T \mathbf{J}_{\mathbf{w}_t}(\mathbf{x})) \mathbf{dw} \\ |\langle \mathbf{dw}, \mathbf{dw} \rangle_{\mathbf{g}_{\mathbf{w}_t}}|^2 &= \mathbf{dw}^T \mathbf{g}_{\mathbf{w}_t}(\mathbf{x}) \mathbf{dw} \end{aligned} \quad (2)$$

where $\mathbf{g}_{\mathbf{w}_t}(\mathbf{x}) = \mathbf{J}_{\mathbf{w}_t}(\mathbf{x})^T \mathbf{J}_{\mathbf{w}_t}(\mathbf{x})$ is the metric tensor evaluated at the point $\mathbf{w}_t \in W$ for a single data point, \mathbf{x} . The metric tensor is an $n \times n$ symmetric matrix that allows us to compute the change in network output for a perturbation along any direction in weight space as $\langle \mathbf{dw}, \mathbf{dw} \rangle_{\mathbf{g}_{\mathbf{w}_t}(\mathbf{x})}$. The metric also allows us to compute the infinitesimal change in network output while moving along a path $\gamma(\mathbf{t})$ in weight space as the tangent vector $\psi(t) = \frac{d\gamma(t)}{dt}$.

At every point in weight space, the metric allows us to discover directions \mathbf{dw} of movement that have large or small impact on the output of a network. As we move along a path, $\gamma(t) \subset W$, in weight space, we sample a series of neural networks over time, t . Using the metric we can define a notion of ‘output velocity’, $\mathbf{v} = \frac{df(\mathbf{x}, \gamma(t))}{dt}$, that quantifies the distance a network moves in output space for each local movement along the weight space path $\gamma(t)$. We seek to identify ‘Functionally invariant paths (FIPs)’ in weight space along which the output velocity is minimized for a fixed magnitude change in weight. To do so, we solve the following optimization problem

$$\begin{aligned} \psi^*(t) &= \underset{\frac{d\gamma}{dt}}{\operatorname{argmin}} \langle \frac{d\gamma}{dt}, \frac{d\gamma}{dt} \rangle_{\mathbf{g}_{\gamma(t)}} \\ \text{with } &\langle \frac{d\gamma}{dt}, \frac{d\gamma}{dt} \rangle_I = \epsilon \end{aligned} \quad (3)$$

where we attempt to find a direction to perturb the network, such that it is ϵ units away in the weight space (in the euclidean sense) ($\langle \frac{d\gamma}{dt}, \frac{d\gamma}{dt} \rangle_I = \epsilon$) while minimizing the distance moved in the networks’ output space, given by $\langle \frac{d\gamma}{dt}, \frac{d\gamma}{dt} \rangle_{\mathbf{g}_{\gamma(t)}}$. Here, I is an identity matrix, with the inner product $\langle \frac{d\gamma}{dt}, \frac{d\gamma}{dt} \rangle_I$ capturing the euclidean distance in the weight space [17]. The optimization problem is a quadratic program at each point in weight space. The metric \mathbf{g} is a matrix that takes on a specific value at each point in weight space, and we aim to identify vectors $\psi^*(t) = \frac{d\gamma(t)}{dt}$, that minimize the change in functional output of the network.

We will often amend the optimization problem with a second objective function $L(\mathbf{x}, \mathbf{w})$. We can enumerate paths that minimize the functional velocity in the output space while moving along the gradient of the second objective ($\nabla_{\mathbf{w}}L$). We define a path-finding algorithm that captures the trade off between these two terms.

$$\begin{aligned} \theta^*(t) &= \underset{\frac{d\gamma}{dt}}{\operatorname{argmin}} (\langle \frac{d\gamma}{dt}, \frac{d\gamma}{dt} \rangle_{\mathbf{g}_{\gamma(t)}} + \beta \langle \frac{d\gamma}{dt}, \nabla_{\mathbf{w}}L \rangle_I) \\ \text{with } &\langle \frac{d\gamma}{dt}, \frac{d\gamma}{dt} \rangle_I = \epsilon \end{aligned} \quad (4)$$

where now the first term, $\langle \frac{d\gamma}{dt}, \frac{d\gamma}{dt} \rangle_{\mathbf{g}_{\gamma(t)}}$, identifies functionally invariant directions while the

second term, $\langle \frac{d\gamma}{dt}, \nabla_{\mathbf{w}} L \rangle_I$, biases the direction of motion along the gradient of a second objective and β weighs the relative contribution of the two terms. When $L = 0$, the algorithm merely constructs paths in weight space that are approximately isofunctional ($\theta^*(t) = \psi^*(t)$), i.e. the path is generated by steps in the weight space comprising of networks with different weight configurations while preserving the input-output map. $L(\mathbf{x}, \mathbf{w})$ can also represent the loss function of a second task, for example a second input classification problem. In this case, we identify vectors that simultaneously maintain performance on an existing task (via term 1) while also improving performance on a second task by moving along the negative gradient of the second task loss function, $\nabla_{\mathbf{w}} L$. We think of constructing FIPs with different objective functions ($L(\mathbf{x}, \mathbf{w})$) similar to applying different “operations” to neural networks that identify sub-manifolds in the weight space of the network that accomplish distinct tasks of interest.

To approximate the solution to Eq-4, in large neural networks, we developed a numerical strategy that samples points in an ϵ ball around a given weight configuration, and then performs gradient descent to identify vectors $\theta^*(t)$. In the appendix, we extend the metric formulation to cases where we consider a set of N training data points, \mathbf{X} , and view \mathbf{g} as the average of metrics derived from individual training examples. $\mathbf{g}_{\mathbf{w}} = \mathbf{g}_{\mathbf{w}}(\mathbf{X}) = \sum_{i=1}^N \mathbf{g}_{\mathbf{w}}(\mathbf{x}_i) / N$. The metric, \mathbf{g} , provides a local measure of *output distance* on the Riemannian manifold $(W, \mathbf{g}_{\mathbf{w}})$. At each point in weight space, the metric defines the length, $\langle d\mathbf{w}, d\mathbf{w} \rangle_{\mathbf{g}_{\mathbf{w}}}$, of a local perturbation by its impact on the functional output of the network (Fig. 1A).

Functionally invariant paths alleviate catastrophic forgetting

We first apply the FIP framework to perform continual learning tasks without catastrophic forgetting on a series of image classification tasks with neural networks of increasing size. In catastrophic forgetting problems, we aim to modulate the weights of an existing neural network to achieve high performance on additional image classification tasks without loss of performance on previously learned tasks. A series of algorithms including the elastic weight consolidation (EWC) [18], Gradient Episodic memory (GEM) [19], Optimal Relevance Mapping (ORM)[20] have been developed to address catastrophic forgetting.

To circumvent catastrophic forgetting while learning sequential tasks, we train a neural network on a base task and modulate the weights in the network to accommodate additional tasks by solving the optimization problem in Eq-4, setting $L(\mathbf{x}, \mathbf{w})$ as the classification loss function specified by the additional task while $\langle \frac{d\gamma}{dt}, \frac{d\gamma}{dt} \rangle_{\mathbf{g}_{\text{Task1}}}$ measures distance moved in the networks’ output using the metric from the initial task (in Eq-4 A(ii)). To accommodate the additional tasks, we append output nodes to the base network and solve the optimization problem for a fixed value of β by simultaneously minimizing the distance moved in the networks’ output space (light-blue arrow) corresponding to the first task while maximizing alignment with the gradient of $L(\mathbf{x}, \mathbf{w})$ encoding the classification loss from the second task. In this manner, we construct a Functionally invariant path (FIP) (purple dotted line) in weight space generating a network that performs both Task 1 and Task 2.

To demonstrate performance of the FIP, we applied the framework to perform a canonical two-task sequential learning paradigm where a convolutional neural network (CNN) trained to classify handwritten digits from MNIST (Task 1) is modulated to also recognize ten classes of fashion apparel from the Fashion-MNIST dataset (FMNIST) (Task 2) (Fig. 2A(i)). For this sequential learning task, we use a CNN with 5 layers: 2 convolutional layers, with 32 and 64 convolutional filters each, and 3 fully connected layers - with 600, 120 and 20 nodes each. The network has a total of 1.4 million weights [21, 3]. The MNIST data set is a canonical data set representing 60,000 examples of human hand written digits [22] and the Fashion-MNIST data contains 60,000 images of fashion items[23].

We initially trained the CNN to perform MNIST digit classification with $\sim 98\%$ accuracy

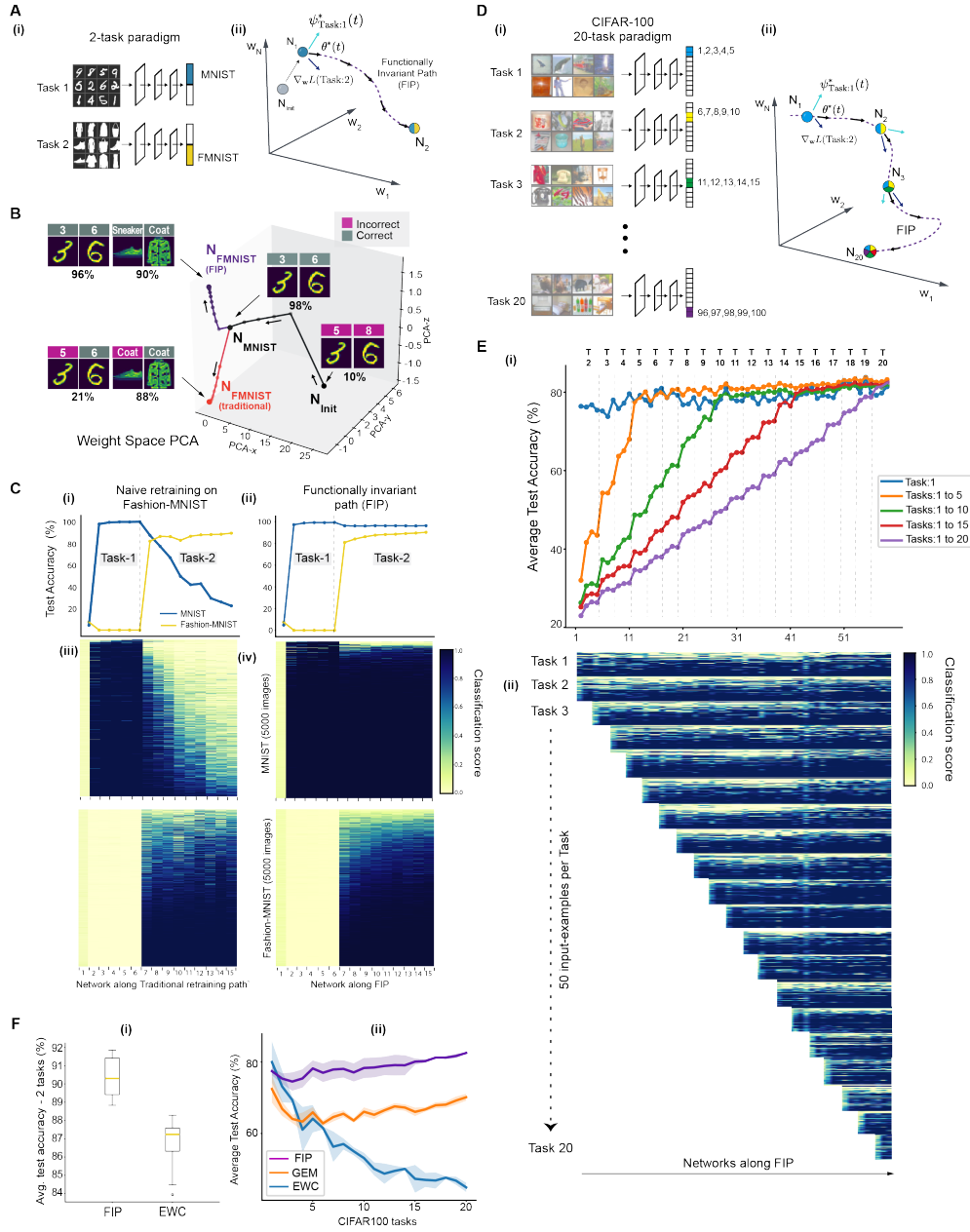


Figure 2: **Networks learn sequential tasks without catastrophic forgetting by traversing FIPs.**

(A)(i) Training neural networks on a 2 task paradigm, with Task-1 being 10-digit recognition from MNIST and Task-2 being 10-item recognition from Fashion-MNIST. (ii) Schematic to construct FIPs in weight space to train networks on two tasks sequentially. (B) 3D lineplot where dots are weight configurations of 5-layered convolutional neural networks (CNNs) in PCA space. Training on two tasks sequentially via conventional approach takes the black followed by red path to reach N_{FMNIST} (traditional), while the path-finding algorithm takes the black followed by purple path to reach N_{FMNIST} (FIP). Images of digits-3,6 are from MNIST and sneaker, coat images are from Fashion-MNIST. Text labels above the image are networks’ predictions and numbers below are the networks’ test accuracy on MNIST and Fashion-MNIST. (C) Test accuracy of networks learning two tasks sequentially by naive retraining on Fashion-MNIST(i) and traversing FIP (ii). Heatmaps capture classification score on 10k test images (5k images from each task) for networks obtained through FIP (iii) and traditional retraining strategy (iv). (D)(i) Neural network with 100 output classes are trained on 20 task paradigm, with every task containing 5 non-overlapping classes of natural images sampled from CIFAR100 dataset. (ii) Schematic to construct FIPs in weight space to train neural networks on 20 sequential tasks. (E)(i) Average test accuracy of networks along FIP while learning 20 sequential tasks. The networks to the right of a dashed line encounter a new task (T-i), referring to the i’th task. (ii) Heatmap displays classification score for networks along FIP on 1k test images, with 50 images sampled from every task. (F) FIP surpasses state-of-art methods in mitigating catastrophic forgetting in 2-task paradigm (i) and 20-task CIFAR100 paradigm (ii). Error bars indicate standard deviation over 5 trials.

using gradient descent based weight optimization (Fig. 2B,C). If we simply re-train the MNIST classification network to classify FMNIST garments through gradient descent on FMNIST, the network rapidly loses accuracy on the MNIST task as accuracy increases on FMNIST (Fig. 2C). In contrast to gradient descent retraining, our FIP algorithm discovers a curved path of networks that simultaneously retain performance on the first task (MNIST), maintaining 98% to 96% test accuracy while reaching 89% performance on the second task (Fashion-MNIST) (Fig. 2C(i)). The networks along the curved FIP path retain their ability to recognize images of digits ‘3’ and ‘6’, while also classifying images of fashion-apparel ‘Sneaker’ and ‘Coat’ from Fashion-MNIST (Fig. 2B).

Functionally invariant paths enable iterative continuous learning

Due to the generality of the framework, the FIP approach naturally scales to learn a longer series of tasks without catastrophic forgetting through iterative application of Eq-4. We applied the FIP to learn 20 sequential image recognition tasks using subsets of the CIFAR100 image database 2D(i) [24]. At each round, we modulate a large CNN, ResNet18, to recognize an additional five object categories in CIFAR100 (2D(i)).

We first train ResNet18 network to obtain 78% accuracy on Task-1 by gradient descent using the Xavier initialization [25] protocol. To learn additional tasks without forgetting, we solve the optimization problem in Eq-4 by setting $L(\mathbf{x}, \mathbf{w})$ as the loss function specified by the incoming new task (Task-i), while $\langle \frac{d\gamma}{dt}, \frac{d\gamma}{dt} \rangle \mathbf{g}_{\text{Task-1:i-1}}$ is set to be the distance moved in output space for a small number of inputs sampled from all the previous tasks (from Task:1 to Task:i-1). In this way, we iteratively construct FIPs in the weight space and obtain networks that simultaneously retain performance on all previous tasks while learning a new task (Fig. 2D).

The FIP strategy achieves high accuracy on incremental tasks broadly across the held-out testing set (Fig. 2E). Having presented all 20 tasks to the network, the FIP algorithm discovers networks that perform at $82.54 \pm 0.17\%$ accuracy while naive re-training performs at $26.86 \pm 1.05\%$ (Supplementary). The FIP approach outperforms other methods that have been introduced to mitigate catastrophic forgetting, specifically Elastic weight consolidation on the 2 task paradigm (Fig. 2F(i)) (FIP: $91 \pm 1.1\%$, EWC: $87 \pm 1.6\%$) and 20-task paradigm (FIP: $82.54 \pm 0.17\%$, EWC: $44.9 \pm 0.01\%$) (Fig. 2F(ii)) and Gradient episodic memory (GEM) with a memory budget of 500 memories from each task previously encountered [18, 19]. While the FIP algorithm has conceptual similarities with EWC, the mathematical generality of the FIP approach allows the approach to scale to perform multiple iterative incremental learning tasks and to explicitly construct functionally invariant paths that span long distances in the weight space. EWC tends to find networks in the vicinity of a previously trained network by computing a local Fisher Information metric.

Network sparsification via path-connected network sets

The critical aspects of the FIP framework is that the framework generalizes beyond sequential task training to address a broad range of machine learning meta-problems by considering a more general set of secondary objective functions. In particular, we next apply the FIP framework to perform sparsification, reducing the number of non-zero weights, of neural networks, which is important for reducing the memory and computational footprint of a network [26]. To sparsify neural networks, we solve Eq-4, the core FIP optimization problem, with a secondary loss function $L(w_t, w, p)$ that measures the euclidean distance between a network and it’s p-sparse projection obtained by setting p% of the networks’ weights to zero.

Using the framework, we discovered a series of sparsified LeNet-300-100 networks with sparsities ranging from 20% to 99.4% that exhibit a high performance on MNIST digit classification [22]. LeNet-300-100 [21] is a multilayer perceptron with two hidden layers consisting of 300 and 100

nodes each, and a total of 484000 non-zero weights. Although most networks randomly sampled from the 99.1% sparse submanifold in the weight space perform poorly on the MNIST task (with test accuracies ranging from 6 to 10%), the FIP algorithm finds a curved path in the weight space from densely connected LeNet (with test accuracy of 98% on MNIST) to networks in the 99.1% sparse submanifold that perform at test accuracies between 96.3% to 96.8% on the MNIST classification task (Fig. 3D). The FIP-discovered networks have diverse inter-layer connectivity structures (Fig. 3F) placing non-zero weights (black vertical bars) in distinct locations. While the FIP solutions vary in their local architectures, there are also patterns across networks. Specifically, across the space of sparse solutions $99.2\pm 0.2\%$ and $98.4\pm 0.3\%$ of the weights between layers 1-2 and 2-3 respectively are zeroed out, while only $52\pm 4\%$ of the weights between layers 3-4 are zeroed out. The differential sparsification across different layers indicates that connections between the first few layers may contain more redundancy than the later layers.

The sparse networks discovered by traversing FIPs have a higher task-performance than the ones discovered through prune-retrain cycles employed within frameworks like the lottery ticket hypothesis (LTH) [27](Fig. 3B). Across a wide range of sparsities (from 20% to 99.4%), FIP discovers networks that are comparable in test accuracy to those obtained by LTH. The FIP also discovers extremely sparse networks with high-performance. The FIP method finds a 99.4% sparse network performing at an accuracy of $96\pm 0.6\%$, while the LTH strategy finds a 99.4% sparse network performing at $91\pm 3\%$ on the MNIST dataset.

The FIP algorithm scales to discover sparse counterparts of CNN networks with multiple layers and skip connections. We applied the FIP framework to sparsify the ResNet-20 architecture [28] with twenty convolutional layers, trained to recognize images of automobiles, animals and man-made structures from the CIFAR-10 dataset. Although most networks sampled from the 93% sparse submanifold of ResNet20 networks perform at accuracies between 18 to 30% on CIFAR10, an FIP constructed from a dense, trained ResNet20 network to the 93% sparse submanifold identifies high performance sparse ResNet20 networks with accuracies between 82 to 84.7% on CIFAR10.

Like the LeNet example, the inter-layer connectivity of sparse ResNet-20 networks are distinct locally, but have globally conserved patterns. For instance, the weights between layers 2 to 19 have an average inter-layer sparsity of 85% while having a maximum sparsity of 99.2%, present between layers 18-19 (penultimate layer), across all sparsified ResNet20 networks (in Fig. 3G, we find that) while the weights between layer 1-2 (first 2 layers) and the layers 19-20 (last 2 layers) are least sparsified (41% and 24% sparse respectively). The differential sparsification across different layers points to the fact that the redundancy in ResNet-20 architectures is encoded primarily between layers 3 and 18. The FIPs discover high performance sparse ResNet20 networks on a wide range of sparse submanifolds (from 20% to 95%) that are at par with the prune-retrain techniques like Lottery ticket hypothesis (LTH) [27].

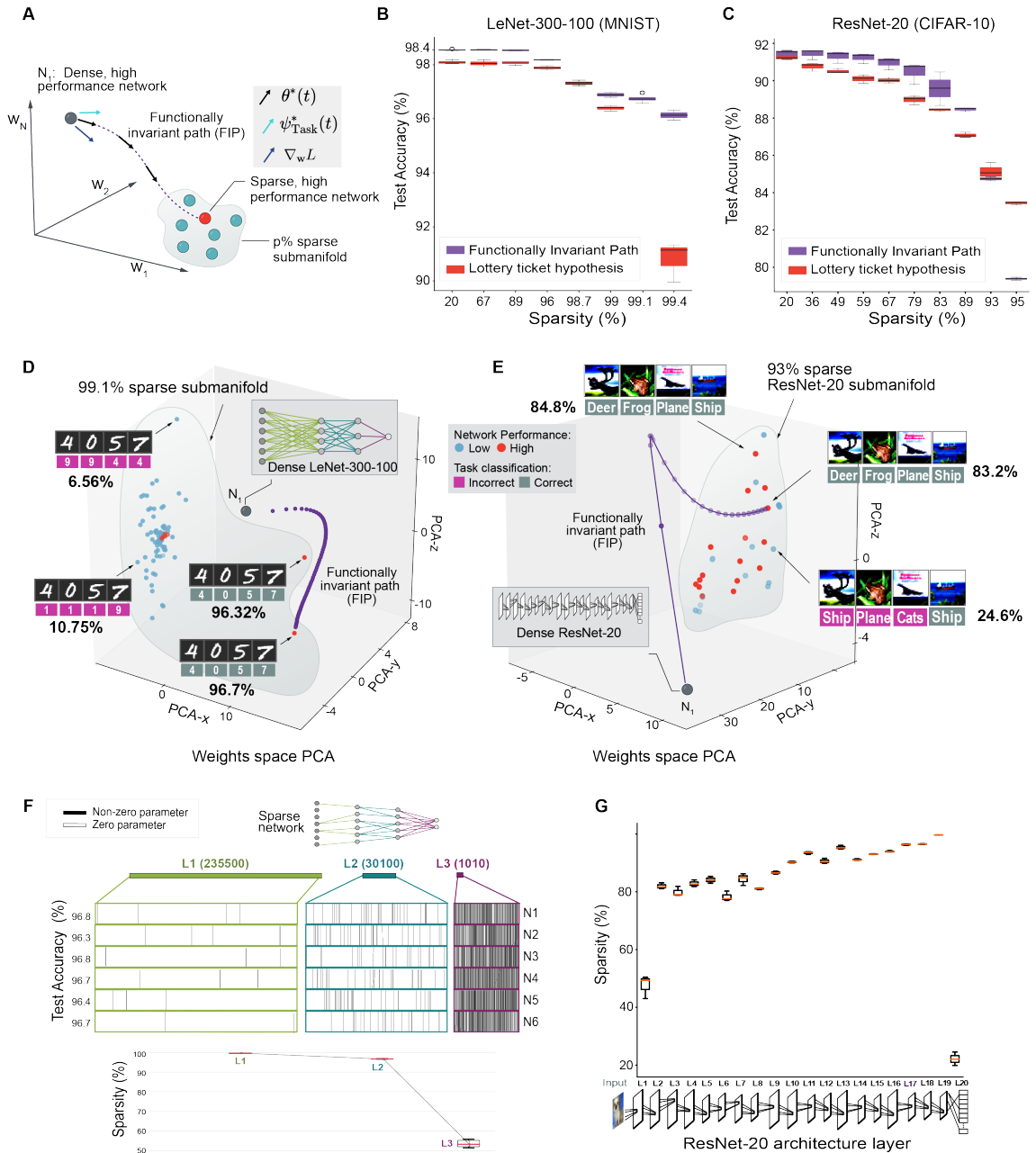


Figure 3: **Sparse networks discovered by traversing FIPs in the weight space.** (A) Schematic to construct FIP from N_1 to $p\%$ sparse submanifold. (B, C) Performance of sparse networks discovered by FIPs (purple) and Lottery ticket hypothesis (red) across a wide range of sparsities on MNIST (B) and CIFAR-10 (C). (D) Scatterplot where the dots are weight configurations of LeNet-300-100 networks in PCA space. The FIP (purple line) beginning from N_1 (grey dot) discovers high-performance LeNet's in the 99.1% sparse submanifold (red dots). Blue dots are random sparse networks in the 99.1% sparse submanifold. Digits-4,0,5,7 are from MNIST, text-labels below the image are network predictions and the number below is the networks' test accuracy on MNIST. (E) Scatterplot where the dots are weight configurations of ResNet-20 networks in PCA space. The FIP beginning at N_1 (grey dot) discovers high-performance ResNet-20 networks in the 93% sparse submanifold (red dots). Blue dots are random sparse networks in 93% sparse submanifold. Deer, frog, plane, ship images are from CIFAR-10, text-labels below the image are network predictions and the number adjacent is the networks' test accuracy on CIFAR10. (F) Sparse LeNet connectivity visualized by plotting vertical lines in color-coded rows to represent non-zero weights. (Below) Boxplot shows sparsity across LeNet's layers. (G) Boxplot shows the sparsity across ResNet-20's layers (over $n=6$ sparsified ResNet's). The cartoon below depicts the ResNet-20 architecture.

Path-connected sets of networks confer robustness against adversarial attack

The path connected sets of networks generated by the FIP can also be applied to perform inference and increase the robustness of inference tasks to data perturbation. Although deep networks have achieved remarkable performance on image-recognition tasks, human-imperceptible additive perturbations, known as adversarial attacks, can be applied to an input image and induce catastrophic errors in deep neural networks (Fig. 4B). The FIP algorithm provides an efficient strategy to increase network robustness and mitigate adversarial failure by generating path-connected sets of networks with diverse weights. We, then, apply the path connected network sets to perform robust image classification by averaging their output.

To demonstrate that the FIP algorithm can mitigate adversarial attacks, we trained a 16 layered CNN, VGG16 with 130 million parameters to classify CIFAR10 images with 92% test accuracy. We, then, generated adversarial test images using the projected gradient descent attack strategy. On adversarial test images, the performance of VGG16 dropped to 37% (Fig. 4B, Supplementary). To mitigate the adversarial performance loss, we applied the FIP algorithm to generate an ensemble of functionally invariant networks by setting $L = 0$ in the optimization problem in Eq-4 and setting $\langle \frac{dy}{dt}, \frac{dy}{dt} \rangle_{\mathbf{g}_{\text{CIFAR10}}}$ to be the distance moved in the networks’ output space for CIFAR-10 images. We use the FIP ensemble to classify images by summing the ‘softmaxed’ outputs of the ensemble.

Using an ensemble of ten networks sampled along an FIP, we achieve accuracy of 55.61 ± 1.1 % surpassing the performance of the DeepNet ensemble performance (composed of 10 independently trained deep networks) by 20.62% (Fig. 4C). The FIP ensemble’s adversarial performance also surpasses other state of the art ensemble approaches including Adaptive Diversity promoting (ADP, $43.84 \pm 7.8\%$) ensemble and the Fast Geometric Ensembling (FGE, 41.7 ± 0.34) method. The two factors contributing to the FIP ensemble’s robustness are (i) high intra-ensemble weight diversity, calculated by the representation diversity score (Supplementary) and (ii) low coherence (Supplementary) with a trained surrogate network (used to generate adversarial images) (Fig. 4E,F). FIP Networks have a higher representation diversity score in their early processing layers, from Layer 1 to layer 6, when compared to the DeepNet ensemble, indicating that individual networks in the FIP ensemble extract different sets of local features from the adversarial image, preventing networks to rely on similar spurious correlations for image classification.

Generating path-connected sets of language models through iterative traversal of weight space paths

FIPs for natural language processing

Conceptually, the most important aspect of the FIP framework is that it unifies a series of machine learning meta-tasks (continual learning, sparsification) into a single mathematical framework. Mathematically, when we solve Equation 4 with a given secondary loss function, we move an existing network $\mathbf{w}(\mathbf{0})$ along a path in weight space generating a new network $\mathbf{w}(\mathbf{t})$ where the parameter t increments the length of a path. Each additional loss function generates a new transformation of a base network, for example, generating a network adjusted to accommodate an additional data analysis problem or a secondary objective like sparsification. Network transformation maps can be iterated and applied to generate a family of neural networks optimized for distinct sub-tasks. The resulting path connected set of neural networks can then be queried for networks that achieve specific user goals or solve additional machine learning problems.

The problem of customization is particularly important for transformer networks that have recently emerged as state of the art architectures in natural language processing [29, 30, 31, 32]. We applied the iterative FIP framework to generate a large number of natural language processing networks customized for different sub-tasks and sparsification goals. Transformer networks incorporate

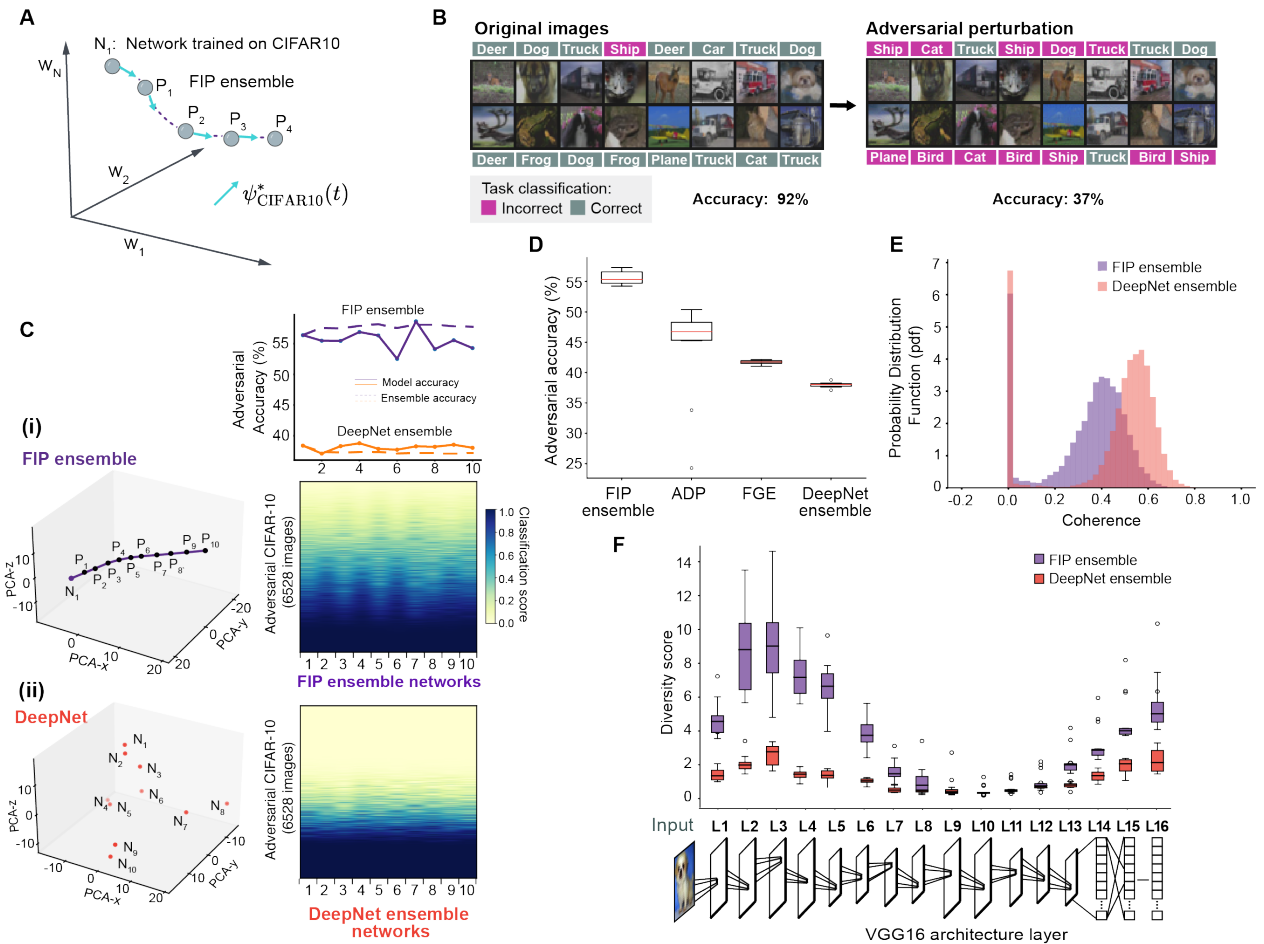


Figure 4: FIPs in weight space generate ensembles of networks that confer adversarial robustness (A) Schematic to generate FIP ensemble (P_1, \dots, P_4) by sampling networks along FIP (purple dotted line) beginning at network- N_1 . FIP is constructed by identifying a series of weight perturbations that minimize the distance moved in networks' output space. (B) Original CIFAR10 images (left) and Adversarial CIFAR-10 images (right) are shown. The text-labels (left, right) above the images are predictions made by a network trained on CIFAR-10. Trained networks' accuracy on the original and adversarial images are shown below. (C) (Top) Line-plot (solid) shows the individual network performance on adversarial inputs, (dashed) shows the joint ensemble accuracy on adversarial inputs, for FIP ensemble (purple) and DeepNet ensemble (orange). (i,ii-Left) FIP ensemble in purple (P_1, P_2, \dots, P_{10}) and DeepNet ensemble in orange (N_1, N_2, \dots, N_{10}) are visualized on weight space PCA. (i,ii-Right) Heatmaps depict classification score of networks in FIP ensemble and DeepNet ensemble on 6528 adversarial CIFAR-10 examples. (D) Boxplot compares adversarial accuracy (over 10k adversarial examples) across different ensembling techniques ($n=3$ trials). (E) Histogram of coherence values for FIP (purple) and DeepNet ensemble (orange). (F) Boxplot shows the ensemble diversity score across VGG16 layers over $n=1000$ CIFAR10 image inputs. The cartoon below depicts the VGG16 network architecture.

layers of attention heads that provide contextual weight for positions in a sentence. Transformer networks are often trained on a generic language processing task like sentence completion where the network must infer missing or masked words in a sentence. Models are, then, fine tuned for specific problems including sentiment analysis, question answering, text generation, and general language understanding [29]. Transformer networks are large containing hundreds of millions of weights, and so model customization can be computationally intensive.

We applied the FIP framework to perform a series of model customization tasks through iterative application of FIP transformations on distinct goals. The BERT network has a total of twelve layers, or transformer blocks, with 12 self-attention heads in each layer and a total of 110 million parameters [33]. Using the FIP framework, we applied two operations (Continual Learning (CL), Compression (Co)) sequentially to BERT models trained on a range of language tasks, by constructing FIPs in the BERT weight space using different objective functions ($L(\mathbf{x}, \mathbf{w})$) while solving the optimization problem in Eq-4. We, first, demonstrated that the FIP framework allowed us to generate versions of the base BERT model that are customized for single-sub-tasks. For example, we sparsified BERT, generating networks with 20 – 80% weights set to zero (Fig. 5A). Similarly, we applied the FIP to adjust the base BERT model, trained on sentence completion, to perform sentiment analysis on YELP and IMDB movie reviews.

Next, we demonstrated that we could apply the operations CL and Co in sequence. Beginning with the BERT base model, we applied the FIP model to generate networks that could perform YELP and IMDB sentiment analysis, and then compressed the resulting networks to generate 6 distinct networks with sparsity ranging from 10 – 60% where all sparsified networks maintained performance on the sentiment analysis tasks (Fig. 5C). We, then, performed the same operations but changed the order of operations. We, first, sparsified the base BERT model to the same six sparsifications and, then, applied the CL operation to sub-train the resulting models on IMDB sentiment analysis. The models generated through application of CL Co(w) and Co CL(w) achieved similar functional performance in terms of sparsification and task performance but had distinct weight configurations.

In total, we used the FIP framework to generate networks using a set of different natural language tasks and compression tasks yielding a path-connected set of 300 BERT models. The 300 networks define a sub-manifold of weight space that contains models customized for distinct sub-tasks. The sub-manifold, then, provides a computational resource for solving new problems. We can query the resulting FIP sub-manifold with unseen data by using perplexity (Supplementary) as a measure of a networks intrinsic ability to separate an unseen data set. Using perplexity, we queried the FIP sub-manifold of BERT networks with IMDB data and Wikitext data. We found that the distinct language data sets achieve minimal perplexity on different classes of networks. Wikitext obtains optimal performance on CoCL networks while IMDB achieves optimal performance on CLCo networks. These results demonstrate that the FIP framework can generate diverse sets of neural networks by transforming networks using distinct meta-tasks. The sub-manifolds of weight space can, then, be queried inexpensively to identify networks pre-optimized for new machine learning problems.

Discussion

We have introduced a mathematical theory and algorithm for training path connected sets of neural networks to solve machine learning problems. We demonstrate that path connected sets of networks can be applied to diversify the functional behavior of a network, enabling the network to accommodate additional tasks, to prune weights, or generate diverse ensembles of networks for preventing failure to adversarial attack. More broadly, our mathematical framework provides a useful conceptual view of neural network training. We view a network as a mathematical object

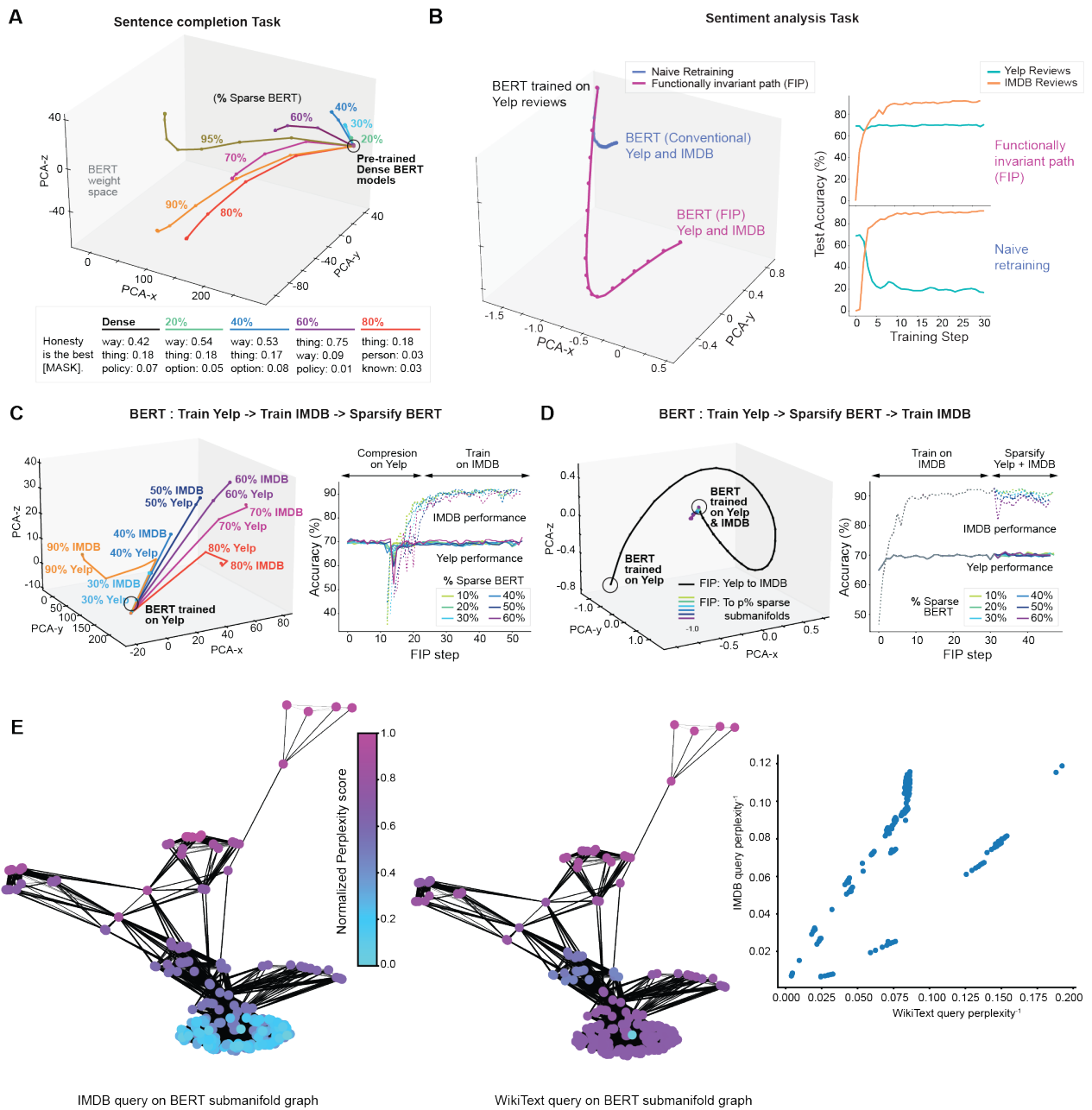


Figure 5: FIPs in large transformer based language model (BERT) weight space. (A, B-C-D (left)) 3D lineplot where dots are weight configurations of 12-layered BERT models with 12 attention heads per layer in PCA space. (A) FIP from pre-trained dense BERT (black circle) discovers high-performance sparse counterparts (labeled p% sparse BERT, where $p \in [20, 30, \dots, 95]$). Table shows "Fill in the Mask" training sample and sparse BERT predictions of the masked word alongside the confidence score. (B, left) Yelp-BERT retrained on IMDB using FIP (purple) and naive retraining (blue). (B, right) BERT performance on Yelp and IMDB. (C, left) FIP initially identify high performance sparse BERTs (for sparsities ranging from 10% to 80%) followed by re-training on IMDB. (C, right) BERT accuracy on Yelp (solid) and IMDB (dashed) dataset along the FIP. (D, left) FIP initially retrains BERT on new task (IMDB) and then discovers a range of sparse BERTs. (D, right) BERT accuracy on Yelp (solid) and IMDB (dashed) dataset along the FIP. (E) Graph connected set of 300 BERT models trained on sentence completion on wikipedia and yelp datasets, colored by perplexity scores evaluated using two new query datasets, wikitext and imdb. Nodes correspond to individual BERT models and edges correspond to euclidean distance between BERT models in weight space. (E, rightmost) Scatter plot of inverse perplexity scores for two queries - IMDB and WikiText datasets.

that can be transformed through iterative application of distinct meta operations. Meta-operations move the network along paths within the weight space of a neural network. Thus, we identify path connected sub-manifolds of weight space that are specialized for different goals. These sub-manifolds can be enumerated using the FIP algorithm and then queried as a computational resource and applied to solve new problems (Fig. 5E).

Fundamentally, our work exploits a parameter degeneracy that is intrinsic to large mathematical models. Previous work has demonstrated that large statistical models often contain significant parameter degeneracy [34] leading to ‘flat’ objective functions [35, 36, 37]. Recent work in physics has demonstrated that physical models with large numbers of parameters often contain parameter degeneracy such that model parameters can be set to any value within a sub-manifold of parameter space without loss of accuracy in predicting experimental data [34]. Mathematically, in the supporting materials we show that the neural networks that we analyze have mathematical signatures of parameter degeneracy after training, through spectral analysis of the metric tensor. Modern deep neural networks contain large numbers of parameters that are fit based on training data, and so are related mathematical objects to physical models with large numbers of parameters set by experimental data, and in fact, exact mappings between statistical mechanics models and neural networks exist [38]. Spectral analysis demonstrates that the weight space contains significant sub-spaces where movement of parameters causes insignificant change in network behavior. Our FIP algorithm explores these degenerate sub-spaces or sub-manifolds of parameter space. Implicitly we show that exploration of the degenerate sub-space can find regions of flexibility where parameters can accommodate a second task (a second image classification task) or goal like sparsification. We apply basic methods from differential geometry to identify and traverse these degenerate sub-spaces. In the Supporting Materials we show that additional concepts from differential geometry including the covariant derivative along a weight space path can be applied to refine paths by minimizing not only the velocity along a weight space path but also acceleration.

Broadly, our results shift attention from the study of single networks to the path-connected sets of neural networks. Biological systems have been hypothesized to explore a range of effective network configurations due to both fluctuation induced drift and modulation of a given network by other sub-systems within the brain. By shifting attention from networks as single configurations or points in weight space to exploring sub-manifolds of the weight space, the FIP framework may help illuminate a potential principle of flexible intelligence and motivate the development of mathematical methods for studying the local and global geometry of functionally invariant solution sets to machine learning problems [5, 39].

References

- [1] D. Silver, *et al.*, *nature* **550**, 354 (2017).
- [2] J. Jumper, *et al.*, *Nature* **596**, 583 (2021).
- [3] A. Krizhevsky, I. Sutskever, G. E. Hinton, *Advances in neural information processing systems* **25** (2012).
- [4] N. Sünderhauf, *et al.*, *The International journal of robotics research* **37**, 405 (2018).
- [5] S. Smale, *The mathematical intelligencer* **20**, 7 (1998).
- [6] T. S. Lee, D. Mumford, *JOSA A* **20**, 1434 (2003).
- [7] M. McCloskey, N. J. Cohen, *Psychology of learning and motivation* (Elsevier, 1989), vol. 24, pp. 109–165.

- [8] R. Ratcliff, *Psychological review* **97**, 285 (1990).
- [9] P. Y. Simard, Y. A. LeCun, J. S. Denker, B. Victorri, *Neural networks: tricks of the trade* (Springer, 1998), pp. 239–274.
- [10] D. E. Rumelhart, G. E. Hinton, R. J. Williams, *nature* **323**, 533 (1986).
- [11] J. Minxha, R. Adolphs, S. Fusi, A. N. Mamelak, U. Rutishauser, *Science* **368**, eaba3313 (2020).
- [12] W. Mau, M. E. Hasselmo, D. J. Cai, *Elife* **9**, e63550 (2020).
- [13] C. Stringer, *et al.*, *Science* **364**, eaav7893 (2019).
- [14] S.-i. Amari, *Information geometry and its applications*, vol. 194 (Springer, 2016).
- [15] I. Benn, R. Tucker, *An introduction to spinors and geometry with applications in physics* (Adam Hilger Ltd, 1987).
- [16] D. H. Mache, J. Szabados, M. G. de Bruin, *Trends and Applications in Constructive Approximation*, vol. 151 (Springer Science & Business Media, 2006).
- [17] E. W. Weisstein, <https://mathworld.wolfram.com/> (2014).
- [18] J. Kirkpatrick, *et al.*, *Proceedings of the national academy of sciences* **114**, 3521 (2017).
- [19] D. Lopez-Paz, M. Ranzato, *Advances in neural information processing systems* **30** (2017).
- [20] P. Kaushik, A. Gain, A. Kortylewski, A. Yuille, *arXiv preprint arXiv:2102.11343* (2021).
- [21] Y. LeCun, P. Haffner, L. Bottou, Y. Bengio, *Shape, contour and grouping in computer vision* (Springer, 1999), pp. 319–345.
- [22] Y. LeCun, L. Bottou, Y. Bengio, P. Haffner, *Proceedings of the IEEE* **86**, 2278 (1998).
- [23] H. Xiao, K. Rasul, R. Vollgraf, *arXiv preprint arXiv:1708.07747* (2017).
- [24] G. M. van de Ven, H. T. Siegelmann, A. S. Tolias, *Nature communications* **11**, 1 (2020).
- [25] X. Glorot, Y. Bengio, *Proceedings of the thirteenth international conference on artificial intelligence and statistics* (JMLR Workshop and Conference Proceedings, 2010), pp. 249–256.
- [26] D. Blalock, J. J. G. Ortiz, J. Frankle, J. Gutttag, *arXiv preprint arXiv:2003.03033* (2020).
- [27] J. Frankle, M. Carbin, *arXiv preprint arXiv:1803.03635* (2018).
- [28] K. He, X. Zhang, S. Ren, J. Sun, *Proceedings of the IEEE conference on computer vision and pattern recognition* (2016), pp. 770–778.
- [29] A. Vaswani, *et al.*, *Advances in neural information processing systems* **30** (2017).
- [30] T. Brown, *et al.*, *Advances in neural information processing systems* **33**, 1877 (2020).
- [31] Y. Liu, *et al.*, *arXiv preprint arXiv:1907.11692* (2019).
- [32] T. Wolf, *et al.*, *Proceedings of the 2020 conference on empirical methods in natural language processing: system demonstrations* (2020), pp. 38–45.
- [33] J. Devlin, M.-W. Chang, K. Lee, K. Toutanova, *arXiv preprint arXiv:1810.04805* (2018).

- [34] B. B. Machta, R. Chachra, M. K. Transtrum, J. P. Sethna, *Science* **342**, 604 (2013).
- [35] S. Hochreiter, J. Schmidhuber, *Neural computation* **9**, 1 (1997).
- [36] S. Hochreiter, J. Schmidhuber, *Advances in neural information processing systems* **7** (1994).
- [37] Y. Tsuzuku, I. Sato, M. Sugiyama, *International Conference on Machine Learning* (PMLR, 2020), pp. 9636–9647.
- [38] P. Mehta, D. J. Schwab, *arXiv preprint arXiv:1410.3831* (2014).
- [39] D. Mumford, A. Desolneux, *Pattern theory: the stochastic analysis of real-world signals* (CRC Press, 2010).